

Connecting Molecular Exchange Dynamics to Stress Relaxation in Phase-Separated Dynamic Covalent Networks

Neil D. Dolinski, Ran Tao, Nicholas R. Boynton, Anthony P. Kotula, Charlie A. Lindberg, Kyle J. Petersen, Aaron M. Forster, and Stuart J. Rowan*



Cite This: *ACS Macro Lett.* 2024, 13, 174–180



Read Online

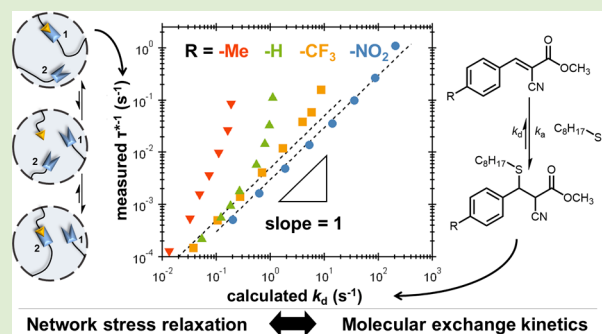
ACCESS |

Metrics & More

Article Recommendations

Supporting Information

ABSTRACT: A suite of phase separated dynamic covalent networks based on highly tunable dynamic benzalcyanoacetate (BCA) thia-Michael acceptors are investigated. In situ kinetic studies on small molecule model systems are used in conjunction with macroscopic characterization of phase stability and stress relaxation to understand how the molecular dynamics relate to relaxation modes. Electronic modification of the BCA unit strongly impacts the exchange dynamics (particularly the rate of dissociation) and the overall equilibrium constant (K_{eq}) of the system, with electron-withdrawing groups leading to decreased dissociation rate and increased K_{eq} . Critically, below a chemistry-defined temperature cutoff (related to the stability of the hard phase domains), the stress relaxation behavior of these phase separated materials is dominated by the molecular exchange dynamics, allowing for networks with a tailored thermomechanical response.



Network stress relaxation ↔ Molecular exchange kinetics

The introduction of dynamic covalent chemistries (DCCs) into cross-linked networks allows for the preparation of robust, intrinsically reprocessable materials (Figure 1a).^{1–3} Such dynamic covalent networks (DCNs), also coined covalent adaptable networks (CANs^{4,5}), have been employed with great success in a wide range of applications spanning biological substrates^{6,7} to additive manufacturing resins.^{8,9} A critical design parameter of DCNs is the selection of the dynamic bonding motifs incorporated into the network, as this determines the exchange mechanism (associative/dissociative), rate of exchange, response to stimulus, and catalyst requirements.^{10–12} As such, a wide swath of DCCs have been explored in materials systems, including transesterification,^{13,14} boronic esters,^{15,16} Diels–Alder reactions,^{17,18} vinylogous urethanes,^{19,20} and many others.^{21,22} While linking molecular exchange dynamics to network response represents a convenient approach to DCN design, there are complications. For instance, it has been demonstrated that a range of design elements, such as component molecular weight,²³ location of dynamic moieties,²⁴ and polymer microphase separation,²⁵ can have dramatic impacts on network relaxation.

While thia-Michael (tM) reactions, the conjugate addition of a thiol to an electron poor alkene, are typically viewed as irreversible reactions, reports have shown that certain Michael acceptors such as maleimides²⁶ and acrylates²⁷ can undergo dynamic exchange with thiols under elevated temperature in the presence of a base. This dynamic behavior can be dramatically enhanced through the use of doubly withdrawn tM acceptors, allowing for exchange under milder conditions.

In particular, benzalcyanoacetate/acetamide (BCA/BCAm) and benzisoxazolone (BiOX) tM acceptors have been developed to undergo dynamic exchange with thiols under ambient conditions (in polar environments), without the need for catalysts (Figure 1b).^{28–32} A signature feature of these species is their strong sensitivity to electronic modifications at the β -phenyl position, with increasing electron-withdrawing character leading to higher values of the equilibrium constant (K_{eq}). This key ability to tune the equilibrium position of BCA/BCAm moieties has been leveraged to prepare a range of materials from hydrogels^{33–35} to responsive dense suspensions^{36,37} with user designed properties. Notably, when prepared as bulk films, BCA-based materials can exhibit an emergent phase separation phenomenon, coined dynamic reaction-induced phase separation (DRIPS), leading to robust mechanical properties despite their ambient dynamic exchange and their relatively low values of K_{eq} (≈ 10 M⁻¹ to 1000 M⁻¹).³⁸ Leveraging DRIPS morphologies has enabled the development of responsive materials systems, such as reprogrammable and self-folding shape memory films³⁸ as well as multipurpose adhesives.³⁹ However, the rational design

Received: November 30, 2023

Revised: January 9, 2024

Accepted: January 17, 2024

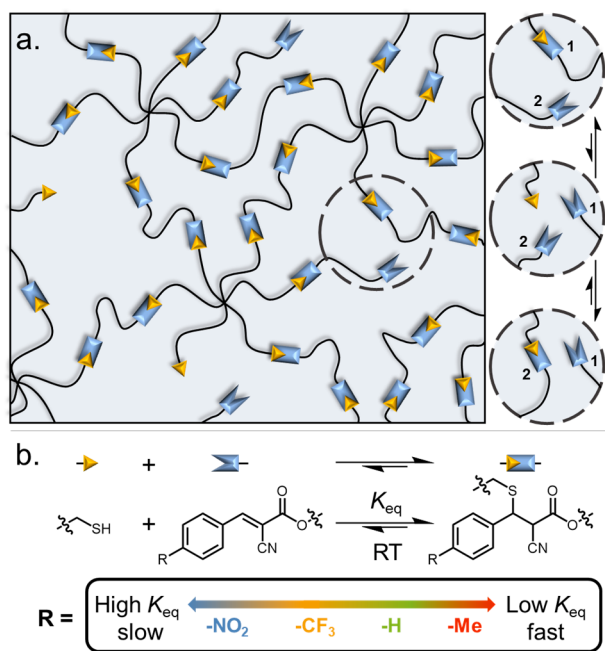


Figure 1. (a) Schematic of a dissociative dynamic covalent network. (b) Representative structures of BCAs and the impact of electronic substituents on K_{eq} and exchange dynamics.

of DRIPS-based materials requires a better understanding of the interplay of the exchange kinetics and the reaction-induced phase separation and how they synergistically impact the macroscopic network relaxation.

To investigate the impact of the electronic modification on exchange dynamics, a series of BCA Michael acceptors bearing a range of withdrawing/donating groups was synthesized (**1R**, where R denotes the substituent at the para-position of the β -phenyl ring). The model compounds were equilibrated with 1-octanethiol in deuterated dimethyl sulfoxide (DMSO- d_6), and their equilibration kinetics were monitored via in situ NMR spectroscopy (Figure 2a). As previously demonstrated, the electronics directly influence the overall reaction equilibrium, with stronger withdrawing character leading to a higher extent of dynamic bond formation (**1OMe** < **1Me** < **1H** < **1Cl** < **1CF₃** < **1NO₂**, Figure 2b), ranging dramatically from 30% to 90% bond formation (@ 100 mM equimolar conditions). This variation in K_{eq} is well described by Hammett σ^+ parameters (Figure S1), in agreement with a recent report.³²

By fitting the measured decay with a dynamic equilibrium model (second order association and first order dissociation; see SI for full information), rate constants could be extracted. The rate of dissociation (k_d) is primarily affected by the electronic nature of the R group, with the fastest dissociation constants ($\approx 10 \text{ h}^{-1}$) for the donating **1OMe** and the slowest ($\approx 0.01 \text{ h}^{-1}$) for the strongly withdrawing **1NO₂** at 25 °C (Figure 2c). This 1000 \times change in k_d signifies a wide range of tunability for the lifetime of the dynamic bonds ($1/k_d$) that can be achieved by manipulating the substituent electronics. In contrast, electronic modifications yield significantly less impact on the association constant, k_a (ranging from $\approx 30 \text{ M}^{-1} \text{ h}^{-1}$ to $80 \text{ M}^{-1} \text{ h}^{-1}$). This implies that the changes in the equilibrium constants for BCA species are primarily driven by dissociation kinetics, which directly translates to the bond lifetime in dynamic material systems. Interestingly, it has been recently reported that electronic modifications of (structurally similar)

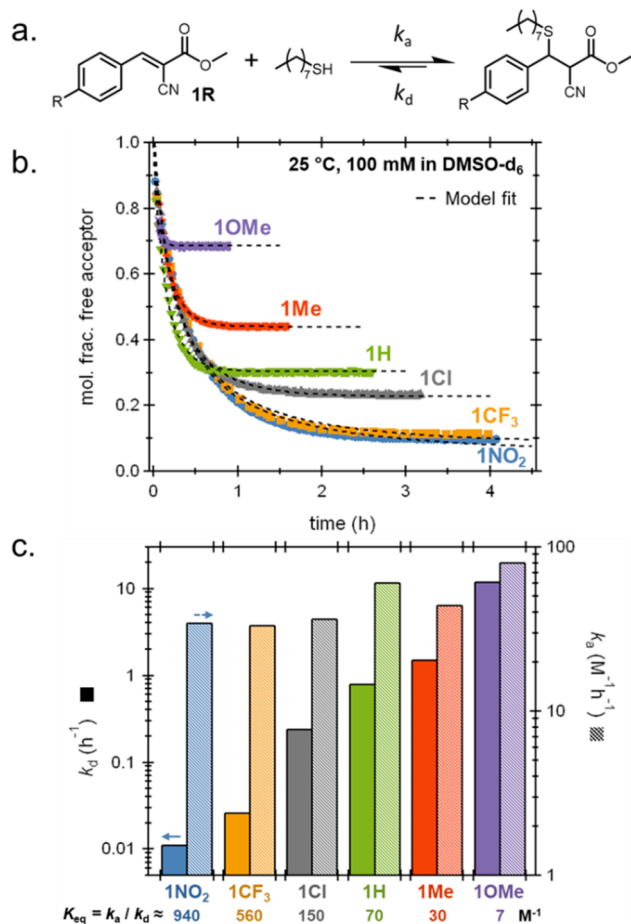


Figure 2. (a) Chemical structures of small molecule BCA analogues (**1R**) used for kinetic studies. (b) Kinetic traces measured at 25 °C for each system. (c) Rate constants extracted from the fits of the room temperature kinetic traces (rate constant standard error <2%).

BCAm acceptors result primarily in changes to k_a rather than k_d (a 20 \times vs 6 \times change across the range in aqueous conditions, respectively).³³ Together, these results highlight how relatively minor modifications to the acceptor structure can lead to significant changes in the exchange behavior.

To extract the activation energies of association/dissociation in these model small molecule systems, kinetic experiments were carried out over several temperatures from 20 to 45 °C (Figures S2–S8). As expected, the activation energy for the association reaction was found to be $\approx 41 \text{ kJ/mol}$ irrespective of electronic modifications, while the activation energy of dissociation ranged from 79 kJ/mol for **1OMe** to 138 kJ/mol for **1NO₂** (increasing gradually with withdrawing ability, Table S1 and Figure S9).

To translate the small molecule studies to DCNs, a series of ditopic tM acceptors (**2R**) were synthesized using a triethylene glycol core, following a previously reported method.³⁸ To form the networks, a stoichiometric mixture (relative to functional groups) of **2R** and a hexathiol cross-linker, dipentaerythritol hexakis(3-mercaptopropionate) (DPHMP), shown in Figure 3a, was mixed in chloroform and cast into Teflon dishes. The hexathiol was chosen for this work to expand the rubbery plateau of the DN-R samples relative to prior studies.³⁸ After thorough drying, the films were compression molded to afford the desired dynamic network (DN-R). As shown in Figure 3b, increasing withdrawing character leads to an increase in glass

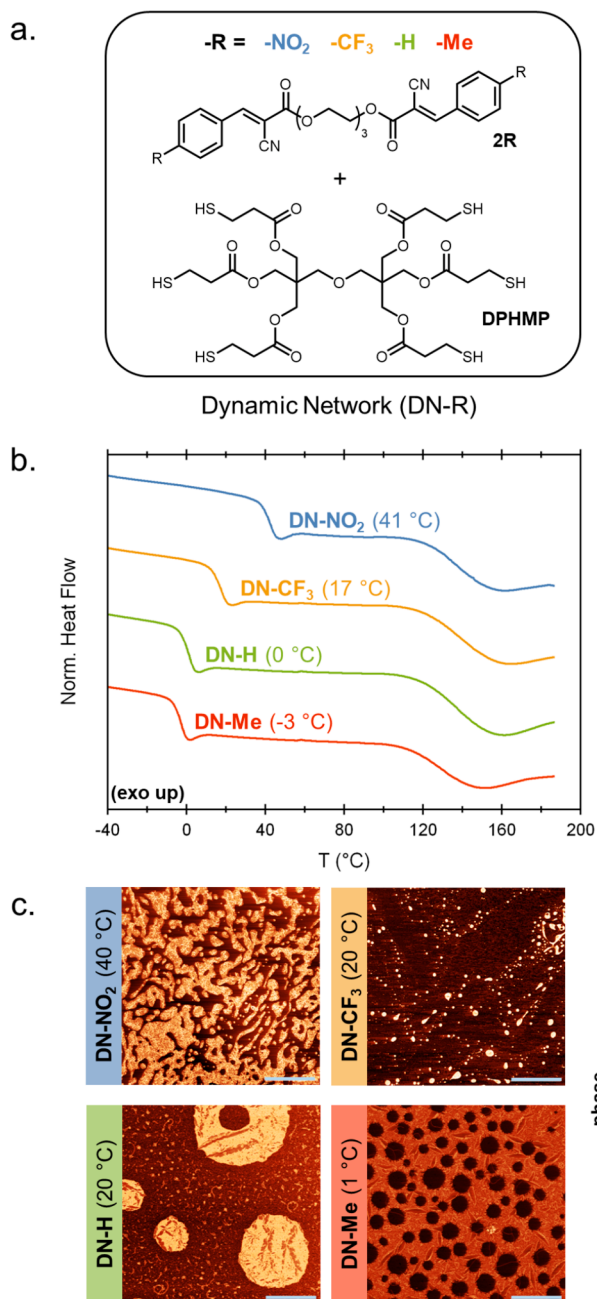


Figure 3. (a) Chemical structures of the monomers used to form the dynamic thia-Michael networks, DN-R. (b) Differential scanning calorimetry (DSC) thermograms, where values indicate the glass transition temperature (T_g), and the second heating scan is shown (ramp rate 10 °C/min). (c) AFM phase images for each network (2 μ m scalebar); height images shown in Figure S12. Phase range (x - y degrees): DN-NO₂ (0–92), DN-CF₃ (0–85), DN-H (0–29), and DN-Me (0–89).

transition temperature (from –3 to 41 °C). Notably, a second endothermic transition at elevated temperature (\approx 120 °C) was observed for DN-Me, DN-H, DN-CF₃, and DN-NO₂, which is a signature indication of the presence of DRIPS.

To visualize the DRIPS morphology, atomic force microscopy (AFM) was carried out (Figures 3c and S12–S16). To ensure optimal phase contrast, imaging was carried out over a range of temperatures (in most cases, contrast was maximized near T_g). Remarkably, a wide array of DRIPS morphologies (hard phase, bright) was found, indicating that

the substituent at the β -phenyl position is a key parameter in determining phase morphology. Despite the obvious impact of electronics on the final morphology, exact trends remain elusive, implying that secondary design parameters (kinetics, solubility, steric bulk, etc.) play important roles in the formation of DRIPS domains. Interestingly, an inverted morphology (isolated low T_g domains) was found in the DN-Me films (the most donating and lowest K_{eq} network). This morphology, in combination with the low phase contrast, implies that the two phases of DN-Me exhibit a much smaller difference in modulus than the other DN-R samples.⁴⁰

To investigate the effect of the dynamic bond exchange kinetics and phase morphologies on the material macroscopic relaxation, stress relaxation experiments were performed in the temperature range of 60 to 150 °C using a strain-controlled shear rheometer. Prior to the measurement at each test temperature, the samples were heated to well above the upper phase transition temperature to erase any hard phase domains or thermal history and were then cooled to each test temperature at a constant rate of 10 °C/min. Once the sample was equilibrated at the test temperature (a minimum of 30 min), a step strain within the linear viscoelastic range was applied, and stress relaxation was recorded (Figures 4a and S18–S21). For all DN-R samples investigated, the data were well described by a stretched exponential fit (eq 1):

$$\frac{G(t)}{G_0} = e^{-(t/\tau^*)^\beta} \quad (1)$$

where G_0 is the starting modulus (as measured at 0.1 s); τ^* is the characteristic relaxation time; and β is the stretching exponent. In all but the highest temperature measurements, values of β primarily ranged from 0.8 to 0.9, suggesting a narrow breadth of the relaxation time distribution.⁴¹ Interestingly, for lower testing temperatures in DN-H, DN-CF₃, and DN-NO₂, the measured τ^* values were found to follow Arrhenius behavior, with calculated activation energy values ranging from 112 to 138 kJ/mol for DN-H to DN-NO₂, respectively. The extracted relaxation activation energies, as well as the measured $\ln(\tau_0)$ values (Arrhenius prefactor), were found to scale linearly with the calculated activation energy of dissociation from small molecule studies, an ideal behavior for bond-mediated relaxation (Figure S22). In contrast, DN-Me was also found to behave in an Arrhenius fashion within the measured range, albeit with an unexpectedly high activation energy of \sim 182 kJ/mol. This strongly temperature dependent behavior is linked to the breakdown of network connectivity, leading to significant decreases in viscosity at considerably lower temperatures than the other studied networks (Figure S23), implying large changes in structure between measurements, as expected for weak dissociative bonds.⁴²

To directly relate the relaxation data to the molecular exchange dynamics, the measured τ^* values were plotted against the calculated dissociation rate (from NMR) for each DN-R. For an ideal dynamic bond-mediated system, τ^* is directly proportional to the bond lifetime ($\tau^* \propto 1/k_b$), resulting in a slope of 1 in Figure 4b. At lower temperatures (corresponding to low k_d values), DN-NO₂, DN-CF₃, and DN-H exhibit this ideal behavior until a deviation occurs at a certain temperature (T_{dev}) as indicated by the arrows in Figure 4b. Intuitively, T_{dev} increases with electron-withdrawing character (and therefore bond strength), from 100 to 130 to 160 °C for DN-H, DN-CF₃, and DN-NO₂, respectively. In the

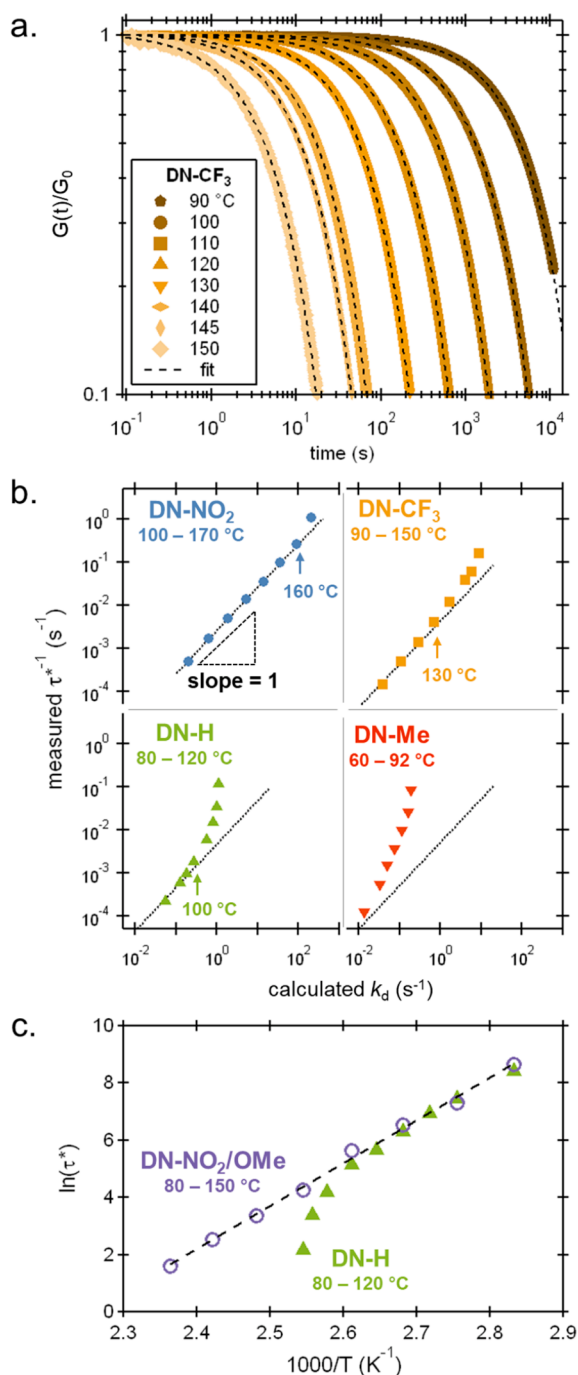


Figure 4. (a) Stress relaxation measurements for DN-CF₃. In all cases, the data are well-fit by a stretched relaxation model. (b) Comparison of measured τ^* values from stress relaxation experiments and calculated rates of dissociation from NMR kinetic studies. Onset of deviation is labeled with an arrow and temperature (in °C). (c) Mixed acceptor network DN-NO₂/OMe showing an enhanced region of Arrhenius response (dashed line) relative to DN-H with similar relaxation time scale.

case of DN-Me (the only example with an inverted phase morphology), the data were found to deviate from the ideal trajectory across all of the measured temperatures.

One of the key advantages of BCA tM acceptors is their broad tunability; however, as demonstrated by the stress relaxation experiments, when targeting faster exchange times (donating groups and lower K_{eq}), the window of well-

controlled Arrhenius relaxation is significantly limited. This issue can potentially be addressed through forming networks from mixtures of ditopic Michael acceptors, combining fast and slow exchange dynamics to selectively tune the exchange rate while relying on the stronger bond to maintain network connectivity. To test this approach, a mixed network sample composed of an equimolar mixture of the slowest (2NO₂) and fastest (2OMe) ditopic tM acceptors was prepared (DN-NO₂/OMe). Similar to the other studied networks, DN-NO₂/OMe was found to exhibit DRIPS via DSC and AFM (Figure S24). At lower temperatures (60 to 100 °C), the hybrid network was found to have nearly identical relaxation time scales as DN-H. However, a notable difference emerged at higher temperatures, where the hybrid material continued to display an Arrhenius behavior well above the breakdown temperature of DN-H (Figure 4c). This result highlights that mixed acceptor systems can be used as a broad platform for ideal, user-defined relaxation behaviors with extended temperature ranges.

To further investigate the cause of these well-defined deviation temperatures, tandem rheology and Raman spectroscopy measurements (rheo-Raman) were carried out, allowing for the direct measurement of the thermal evolution of network chemistry.⁴³ It was previously shown that Raman spectroscopy could estimate the extent of bond formation through the nitrile stretch region (≈ 2220 cm⁻¹ to 2260 cm⁻¹), where peaks corresponding to associated and dissociated Michael acceptors can be readily identified (Figures 5a and S26).³⁸ Due to sample fluorescence, DN-NO₂ and DN-Me were unsuitable for measurement (Figure S27). Samples were first annealed well above the DRIPS phase transition (>150 °C) to effectively clear hard phase domains and then were cooled to 60 °C and subsequently reheated to the starting temperature at a fixed rate of 1 °C/min. As expected, the initial cooling cycle leads to a steady increase in bond formation (points 1–3 in Figure 5b), inducing gelation and DRIPS. Upon heating, however, a pronounced plateau in bonding was observed (points 3–4 in Figure 5b). In both DN-CF₃ and DN-H, this plateau in bonding was found to abruptly decline and close the hysteresis loop at a repeatable onset temperature (T_{onset}), occurring at 130 and 100 °C for DN-CF₃ and DN-H, respectively. The corresponding rheology data show that T_{onset} directly relates to the temperature at which the samples experience flow upon heating (Figure 5c). To ensure that T_{onset} is not determined solely by the cooling conditions, a series of experiments cooling to different set points were performed on DN-CF₃. In all cases, T_{onset} remained unchanged (Figures S29 and S30). Taken together, these data suggest that the plateau region is related to trapped out-of-equilibrium bonds within the hard phase, which are rapidly released upon hard phase softening (above the onset temperature). Notably T_{onset} differs substantially from the DRIPS signature in DSC, potentially highlighting the influence of applied stress. The sudden loss of reinforcement in a network composed of low K_{eq} bonds results in a loss of network integrity. Remarkably, this phase softening temperature (for DN-CF₃ and DN-H) as measured by rheo-Raman closely matches the temperature at which stress relaxation measurements deviate from Arrhenius behavior ($T_{dev} = T_{onset}$). At temperatures below T_{onset} , networks are stabilized by hard phase domains and behave in an Arrhenius fashion, in strong agreement with model exchange kinetics. When heated above T_{onset} the hard phase domains are destabilized, leading to the loss of mechanical integrity.

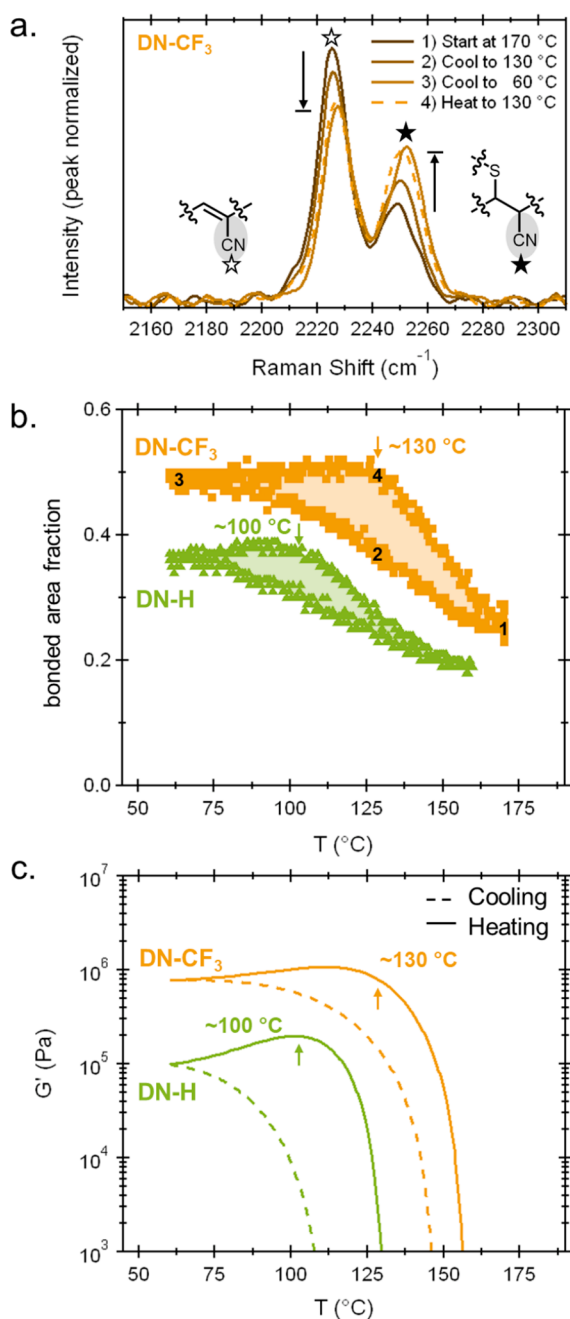


Figure 5. (a) Peaks of interest for determining the extent of bonding using Raman spectroscopy (data shown for DN-CF₃). (b) Hysteresis loops as measured by Raman during a cooling–heating cycle. Onset of peak area reduction on heating is denoted with an arrow. (c) Corresponding temperature ramp rheology data; arrows match placement from Figure 5b.

In summary, dynamic covalent networks based on benzalcyanoacetate (BCA) Michael acceptors are highly sensitive to electronic modifications, giving access to tunable thermomechanical properties. Manipulating the electronics of the BCA dramatically impacts the rate of dissociation, slowing by $\approx 1000\times$ with increasing withdrawing character. Preparing bulk films from ditopic BCA acceptors leads to phase separated networks with thermomechanical properties highly correlated to electronic modification. Comparisons between small molecule exchange dynamics and bulk stress relaxation experiments reveal that despite their relatively low K_{eq} values

the networks show ideal bond-mediated, Arrhenius relaxation up to a chemistry-defined deviation temperature. The network chemistry as measured by rheo-Raman spectroscopy reveals that this deviation temperature is linked to hard phase stability, with hard phase domains trapping out-of-equilibrium bonds and lending reinforcement to the otherwise weak networks. Ongoing research seeks to use filler additions and heat treatment processes to further manipulate DRIPS to access highly controlled phase separated morphologies and network thermomechanical properties.

■ ASSOCIATED CONTENT

Data Availability Statement

All raw data files are available from the corresponding author upon reasonable request.

Supporting Information

The Supporting Information is available free of charge at <https://pubs.acs.org/doi/10.1021/acsmacrolett.3c00717>.

Experimental details, kinetic analysis, as well as additional characterization of DRIPS networks including thermogravimetric analysis, differential scanning calorimetry, atomic force microscopy, stress relaxation, and rheo-Raman (PDF)

■ AUTHOR INFORMATION

Corresponding Author

Stuart J. Rowan – Pritzker School of Molecular Engineering and Department of Chemistry, University of Chicago, Chicago, Illinois 60637, United States; Chemical Science and Engineering Division and Center for Molecular Engineering, Argonne National Laboratory, Lemont, Illinois 60434, United States; orcid.org/0000-0001-8176-0594; Email: stuartrowan@uchicago.edu

Authors

Neil D. Dolinski – Pritzker School of Molecular Engineering, University of Chicago, Chicago, Illinois 60637, United States; orcid.org/0000-0002-2160-8811

Ran Tao – Material Measurement Laboratory, National Institute of Standards and Technology, Gaithersburg, Maryland 20899, United States; Department of Chemical and Biomolecular Engineering, North Carolina State University, Raleigh, North Carolina 27695, United States; orcid.org/0000-0002-5208-7895

Nicholas R. Boynton – Pritzker School of Molecular Engineering, University of Chicago, Chicago, Illinois 60637, United States

Anthony P. Kotula – Material Measurement Laboratory, National Institute of Standards and Technology, Gaithersburg, Maryland 20899, United States; orcid.org/0000-0002-0830-2869

Charlie A. Lindberg – Pritzker School of Molecular Engineering, University of Chicago, Chicago, Illinois 60637, United States; orcid.org/0000-0001-8391-4753

Kyle J. Petersen – Pritzker School of Molecular Engineering, University of Chicago, Chicago, Illinois 60637, United States

Aaron M. Forster – Material Measurement Laboratory, National Institute of Standards and Technology, Gaithersburg, Maryland 20899, United States; orcid.org/0000-0002-5323-2468

Complete contact information is available at: <https://pubs.acs.org/doi/10.1021/acsmacrolett.3c00717>

Author Contributions

The manuscript was written by N.D.D. and S.J.R. Experiments were designed by N.D.D., R.T., A.P.K., A.M.F., and S.J.R. Materials were synthesized by N.D.D., N.R.B., C.A.L., and K.J.P. Experiments were performed by N.D.D., R.T., N.R.B., and A.P.K. All authors have given approval to the final version of the manuscript. CRediT: **Neil D Dolinski** conceptualization, formal analysis, investigation, methodology, writing-original draft; **Ran Tao** conceptualization, formal analysis, investigation, methodology, writing-original draft; **Nicholas R. Boynton** investigation, writing-review & editing; **Anthony P. Kotula** formal analysis, investigation, writing-review & editing; **Charlie A. Lindberg** investigation, writing-review & editing; **Kyle J. Petersen** investigation; **Aaron M. Forster** conceptualization, funding acquisition, project administration, supervision, writing-review & editing; **Stuart J. Rowan** conceptualization, funding acquisition, project administration, supervision, writing-review & editing.

Notes

The full description of the procedures used in this paper requires the identification of certain commercial products and their suppliers. The inclusion of such information should in no way be construed as indicating that such products or suppliers are endorsed by NIST, or are recommended by NIST, or that they are necessarily the best materials, instruments, software, or suppliers for the purposes described.

The authors declare no competing financial interest.

ACKNOWLEDGMENTS

This work was supported in part by NIST contract 60NANB15D077, the Center for Hierarchical Materials Design (CHiMaD), and the Division of Materials Research of the NSF (Award #2104694). R.T. acknowledges the National Institute of Standards and Technology for funding (Award No. 70NANB21H106). N.R.B. was supported through a NASA Space Technology Graduate Research Opportunity. This work was partially supported by the University of Chicago Materials Research Science and Engineering Center (MRSEC), which is funded by the National Science Foundation under award number DMR-2011854. Parts of this work were carried out at the Soft Matter Characterization Facility and at the MRSEC Characterization Facility at the University of Chicago (award number DMR-2011854).

REFERENCES

- (1) Rowan, S. J.; Cantrill, S. J.; Cousins, G. R. L.; Sanders, J. K. M.; Stoddart, J. F. Dynamic Covalent Chemistry. *Angewandte Chemie - International Edition* **2002**, *41* (6), 898–952.
- (2) Jin, Y.; Yu, C.; Denman, R. J.; Zhang, W. Recent Advances in Dynamic Covalent Chemistry. *Chem. Soc. Rev.* **2013**, *42* (16), 6634–6654.
- (3) Herbert, K. M.; Schrettl, S.; Rowan, S. J.; Weder, C. 50th Anniversary Perspective: Solid-State Multistimuli, Multiresponsive Polymeric Materials. *Macromolecules* **2017**, *50* (22), 8845–8870.
- (4) Kloxin, C. J.; Scott, T. F.; Adzima, B. J.; Bowman, C. N. Covalent Adaptable Networks (CANs): A Unique Paradigm in Cross-Linked Polymers. *Macromolecules* **2010**, *43* (6), 2643–2653.
- (5) Kloxin, C. J.; Bowman, C. N. Covalent Adaptable Networks: Smart, Reconfigurable and Responsive Network Systems. *Chem. Soc. Rev.* **2013**, *42* (17), 7161–7173.
- (6) Zhang, Y.; Qi, Y.; Ulrich, S.; Barboiu, M.; Ramström, O. Dynamic Covalent Polymers for Biomedical Applications. *Mater. Chem. Front* **2020**, *4* (2), 489–506.

- (7) Rizwan, M.; Baker, A. E. G.; Shoichet, M. S. Designing Hydrogels for 3D Cell Culture Using Dynamic Covalent Crosslinking. *Adv. Healthc. Mater.* **2021**, *10* (12), 2100234.
- (8) Durand-Silva, A.; Cortés-Guzmán, K. P.; Johnson, R. M.; Perera, S. D.; Diwakara, S. D.; Smaldone, R. A. Balancing Self-Healing and Shape Stability in Dynamic Covalent Photoresins for Stereolithography 3D Printing. *ACS Macro Lett.* **2021**, *10* (4), 486–491.
- (9) Robinson, L. L.; Self, J. L.; Fusi, A. D.; Bates, M. W.; Read De Alaniz, J.; Hawker, C. J.; Bates, C. M.; Sample, C. S. Chemical and Mechanical Tunability of 3D-Printed Dynamic Covalent Networks Based on Boronate Esters. *ACS Macro Lett.* **2021**, *10*, 857–863.
- (10) Zhang, V.; Kang, B.; Accardo, J. V.; Kalow, J. A. Structure-Reactivity-Property Relationships in Covalent Adaptable Networks. *J. Am. Chem. Soc.* **2022**, *144* (49), 22358–22377.
- (11) Wanasinghe, S. V.; Dodo, O. J.; Konkolewicz, D. Dynamic Bonds: Adaptable Timescales for Responsive Materials. *Angewandte Chemie - International Edition* **2022**, *61* (50), No. e202206938.
- (12) Marco-Dufort, B.; Iten, R.; Tibbitt, M. W. Linking Molecular Behavior to Macroscopic Properties in Ideal Dynamic Covalent Networks. *J. Am. Chem. Soc.* **2020**, *142* (36), 15371–15385.
- (13) Montarnal, D.; Capelot, M.; Tournilhac, F.; Leibler, L. Silica-like Malleable Materials from Permanent Organic Networks. *Science* (1979) **2011**, *334* (6058), 965–968.
- (14) Self, J. L.; Dolinski, N. D.; Zayas, M. S.; Read De Alaniz, J.; Bates, C. M. Brønsted-Acid-Catalyzed Exchange in Polyester Dynamic Covalent Networks. *ACS Macro Lett.* **2018**, *7* (7), 817–821.
- (15) Hong, S. H.; Kim, S.; Park, J. P.; Shin, M.; Kim, K.; Ryu, J. H.; Lee, H. Dynamic Bonds between Boronic Acid and Alginate: Hydrogels with Stretchable, Self-Healing, Stimuli-Responsive, Remoldable, and Adhesive Properties. *Biomacromolecules* **2018**, *19* (6), 2053–2061.
- (16) Porath, L.; Huang, J.; Ramlawi, N.; Derkaloustian, M.; Ewoldt, R. H.; Evans, C. M. Relaxation of Vitrimers with Kinetically Distinct Mixed Dynamic Bonds. *Macromolecules* **2022**, *55* (11), 4450–4458.
- (17) Chen, X.; Wudl, F.; Mal, A. K.; Shen, H.; Nutt, S. R. New Thermally Remendable Highly Cross-Linked Polymeric Materials. *Macromolecules* **2003**, *36* (6), 1802–1807.
- (18) Zhou, Q.; Sang, Z.; Rajagopalan, K. K.; Sliozberg, Y.; Gardea, F.; Sukhishvili, S. A. Thermodynamics and Stereochemistry of Diels-Alder Polymer Networks: Role of Crosslinker Flexibility and Crosslinking Density. *Macromolecules* **2021**, *54* (22), 10510–10519.
- (19) Denissen, W.; Rivero, G.; Nicolaÿ, R.; Leibler, L.; Winne, J. M.; Du Prez, F. E. Vinylogous Urethane Vitrimers. *Adv. Funct. Mater.* **2015**, *25* (16), 2451–2457.
- (20) Engelen, S.; Wróblewska, A. A.; De Bruycker, K.; Aksakal, R.; Ladmiral, V.; Caillol, S.; Du Prez, F. E. Sustainable Design of Vanillin-Based Vitrimers Using Vinylogous Urethane Chemistry. *Polym. Chem.* **2022**, *13* (18), 2665–2673.
- (21) Ishibashi, J. S. A.; Kalow, J. A. Vitrimeric Silicone Elastomers Enabled by Dynamic Meldrum's Acid-Derived Cross-Links. *ACS Macro Lett.* **2018**, *7* (4), 482–486.
- (22) Orrillo, A. G.; Furlan, R. L. E. Sulfur in Dynamic Covalent Chemistry. *Angewandte Chemie - International Edition* **2022**, *61* (26), No. e202201168.
- (23) Lessard, J. J.; Stewart, K. A.; Sumerlin, B. S. Controlling Dynamics of Associative Networks through Primary Chain Length. *Macromolecules* **2022**, *55* (22), 10052–10061.
- (24) Lindberg, C. A.; Ghimire, E.; Chen, C.; Lee, S.; Dolinski, N. D.; Dennis, J. M.; Wang, S.; de Pablo, J. J.; Rowan, S. J. Exploring the Effect of Dynamic Bond Placement in Liquid Crystal Elastomers. *J. Polym. Sci.* **2023**, DOI: 10.1002/pol.20230547.
- (25) Lessard, J. J.; Scheutz, G. M.; Sung, S. H.; Lantz, K. A.; Epps, T. H.; Sumerlin, B. S. Block Copolymer Vitrimers. *J. Am. Chem. Soc.* **2020**, *142* (1), 283–289.
- (26) Chakma, P.; Rodrigues Possarle, L. H.; Digby, Z. A.; Zhang, B.; Sparks, J. L.; Konkolewicz, D. Dual Stimuli Responsive Self-Healing and Malleable Materials Based on Dynamic Thiol-Michael Chemistry. *Polym. Chem.* **2017**, *8* (42), 6534–6543.

(27) Zhang, B.; Digby, Z. A.; Flum, J. A.; Chakma, P.; Saul, J. M.; Sparks, J. L.; Konkolewicz, D. Dynamic Thiol-Michael Chemistry for Thermoresponsive Rehealable and Malleable Networks. *Macromolecules* **2016**, *49* (18), 6871–6878.

(28) Serafimova, I. M.; Pufall, M. A.; Krishnan, S.; Duda, K.; Cohen, M. S.; Maglathlin, R. L.; McFarland, J. M.; Miller, R. M.; Frödin, M.; Taunton, J. Reversible Targeting of Noncatalytic Cysteines with Chemically Tuned Electrophiles. *Nat. Chem. Biol.* **2012**, *8*, 471.

(29) Zhong, Y.; Xu, Y.; Anslyn, E. V. Studies of Reversible Conjugate Additions. *Eur. J. Org. Chem.* **2013**, *2013* (23), 5017–5021.

(30) Krenske, E. H.; Petter, R. C.; Houk, K. N. Kinetics and Thermodynamics of Reversible Thiol Additions to Mono- and Diactivated Michael Acceptors: Implications for the Design of Drugs That Bind Covalently to Cysteines. *J. Org. Chem.* **2016**, *81* (23), 11726–11733.

(31) Kuhl, N.; Geitner, R.; Bose, R. K.; Bode, S.; Dietzek, B.; Schmitt, M.; Popp, J.; Garcia, S. J.; van der Zwaag, S.; Schubert, U. S.; Hager, M. D. Self-Healing Polymer Networks Based on Reversible Michael Addition Reactions. *Macromol. Chem. Phys.* **2016**, *217*, 2541–2550.

(32) Crolais, A. E.; Dolinski, N. D.; Boynton, N. R.; Radhakrishnan, J. M.; Snyder, S. A.; Rowan, S. J. Enhancing the Equilibrium of Dynamic Thia-Michael Reactions through Heterocyclic Design. *J. Am. Chem. Soc.* **2023**, *145* (26), 14427–14434.

(33) Fitzsimons, T. M.; Oentoro, F.; Shanbhag, T. V.; Anslyn, E. V.; Rosales, A. M. Preferential Control of Forward Reaction Kinetics in Hydrogels Crosslinked with Reversible Conjugate Additions. *Macromolecules* **2020**, *53* (10), 3738–3746.

(34) FitzSimons, T. M.; Anslyn, E. V.; Rosales, A. M. Effect of PH on the Properties of Hydrogels Cross-Linked via Dynamic Thia-Michael Addition Bonds. *ACS Polymers Au* **2022**, *2* (2), 129–136.

(35) Crowell, A. D.; FitzSimons, T. M.; Anslyn, E. V.; Schultz, K. M.; Rosales, A. M. Shear Thickening Behavior in Injectable Tetra-PEG Hydrogels Cross-Linked via Dynamic Thia-Michael Addition Bonds. *Macromolecules* **2023**, *56* (19), 7795–7807.

(36) Jackson, G. L.; Dennis, J. M.; Dolinski, N. D.; Van Der Naald, M.; Kim, H.; Eom, C.; Rowan, S. J.; Jaeger, H. M. Designing Stress-Adaptive Dense Suspensions Using Dynamic Covalent Chemistry. *Macromolecules* **2022**, *55* (15), 6453–6461.

(37) Kim, H.; van der Naald, M.; Dolinski, N. D.; Rowan, S. J.; Jaeger, H. M. Dynamic-Bond-Induced Sticky Friction Tailors Non-Newtonian Rheology. *Soft Matter* **2023**, *19* (35), 6797–6804.

(38) Herbert, K. M.; Getty, P. T.; Dolinski, N. D.; Hertzog, J. E.; de Jong, D.; Lettow, J. H.; Romulus, J.; Onorato, J. W.; Foster, E. M.; Rowan, S. J. Dynamic Reaction-Induced Phase Separation in Tunable, Adaptive Covalent Networks. *Chem. Sci.* **2020**, *11* (19), 5028–5036.

(39) Herbert, K. M.; Dolinski, N. D.; Boynton, N. R.; Murphy, J. G.; Lindberg, C. A.; Sibener, S. J.; Rowan, S. J. Controlling the Morphology of Dynamic Thia-Michael Networks to Target Pressure-Sensitive and Hot Melt Adhesives. *ACS Appl. Mater. Interfaces* **2021**, *13* (23), 27471–27480.

(40) Zhu, J.; Chen, L.-Q.; Shen, J. Morphological Evolution during Phase Separation and Coarsening with Strong Inhomogeneous Elasticity. *Model Simul Mat Sci. Eng.* **2001**, *9*, 499–511.

(41) Johnston, D. C. Stretched Exponential Relaxation Arising from a Continuous Sum of Exponential Decays. *Phys. Rev. B* **2006**, *74*, 184430.

(42) Elling, B. R.; Dichtel, W. R. Reprocessable Cross-Linked Polymer Networks: Are Associative Exchange Mechanisms Desirable? *ACS Cent Sci.* **2020**, *6*, 1488–1496.

(43) Kotula, A. P.; Meyer, M. W.; De Vito, F.; Plog, J.; Hight Walker, A. R.; Migler, K. B. The Rheo-Raman Microscope: Simultaneous Chemical, Conformational, Mechanical, and Microstructural Measures of Soft Materials. *Rev. Sci. Instrum.* **2016**, *87* (10), 105105.